ANALYSIS OF THE AUGUST 7, 1972 WHITE LIGHT FLARE: LIGHT CURVES AND CORRELATION WITH HARD X-RAYS

DAVID M. RUST*

Sacramento Peak Observatory, Air Force Cambridge Research Laboratories, Sunspot, N.M. 88349, U.S.A.

and

FRANK HEGWER

*High Altitude Observatory, National Center for Atmospheric Research**, Boulder, Colo. 80303, U.S.A.*

(Received 2 October, 1974)

Abstract. Cinematic, photometric observations of the 3B flare of August 7, 1972 are described in detail. The time resolution was 2 s; the spatial resolution was 1–2″. Flare continuum emissivity at 4950 Å and at 5900 Å correlated closely in time with the 60–100 keV non-thermal X-ray burst intensity. The observed peak emissivity was 1.5×10^{10} erg cm^{-2} s^{-1} and the total flare energy in the 3900–6900 Å range was $\sim 10^{30}$ erg. From the close temporal correspondence and from the small distance (3″) separating the layers where the visible emission and the X-rays arose, it is argued that the hard X-ray source must have had the same silhouette as the white light flare and that the emission patches had cross-sections of 3–5″. There was also a correlation between the location of the most intense visible emissions near sunspots and the intensity and polarization of the 9.4 GHz radio emission. The flare appeared to show at least three distinct particle acceleration phases: one, occurring at a stationary source and associated with proton acceleration gave a very bluish continuum and reached peak intensity at ~ 1522 UT. At 1523 UT, a faint wave spread out at 40 km s^{-1} from flare center. The spectrum of the wave was nearly flat in the range 4950–5900 Å. Association of the wave with a slow drift of the microwave emission peak to lower frequencies and with a softening of the X-ray spectrum is interpreted to mean that the particle acceleration process weakened while the region of acceleration expanded. The observations are interpreted with the aid of the flare models of Brown to mean that the same beam of non-thermal electrons that was responsible for the hard X-ray bremsstrahlung also caused the heating of the lower chromosphere that produced the white light flare.

In the first two weeks of August, 1972, a series of large flares occurred in McMath region 11976, and at least one of these, the flare that started at 1510 UT on August 7, was a rare white light event. Švestka (1970) has most recently discussed the possible causes of white light flares, and a comprehensive, three volume collection of data on the August flares has been published by Coffey (1973).

In this paper, we describe cinematic, photometric observations of the white light flare. We consider the proposition that the white light emission outlines the region of hard X-ray production in the flare. In an effort to locate the region of particle acceleration, we compare our observations of the visible continuum with hard X-ray, hydrogen-alpha, helium D_3 and microwave radio emissions. In an accompanying paper, Machado and Rust (1974) discuss the spectrum and vertical structure of the optical flare.

* Present address: American Science and Engineering Co., Cambridge, Mass. 02139, U.S.A.

** The National Center for Atmospheric Research is sponsored by the National Science Foundation.

Solar Physics **40** (1975) 141–157.

1. Instrumentation

The Hilltop patrol camera at the Sacramento Peak Observatory isprogrammed to photograph the solar disk on 35 mm film every 10 min, but the rate is increased to once per minute in periods of high activity. On August 7, we obtained pictures at the 10 min rate until 1522 UT when the telescope was switched to the 1 min rate. The details of the instrument are given by DeMastus and Stover (1967). They show the transmission curve of the VG 9 and OG 2 Schott filters used with the system. The resultant passband is 175 Å wide; it is centered at 5900 Å.

The Vacuum Tower Telescope at Sacramento Peak produces a 500 mm diam solar image; the white light flare photographs were taken with a 70 mm Acme camera that captures a 56 mm square portion of this image. Figure 1 shows the resultant transmission curve of the GG 495 and BG 25 filters and Kodak 5460 film used with the system. The passband is 250 Å wide and it is centered at about 4950 Å. During 1972 this system was used to obtain high resolution pictures of large sunspot groups on a

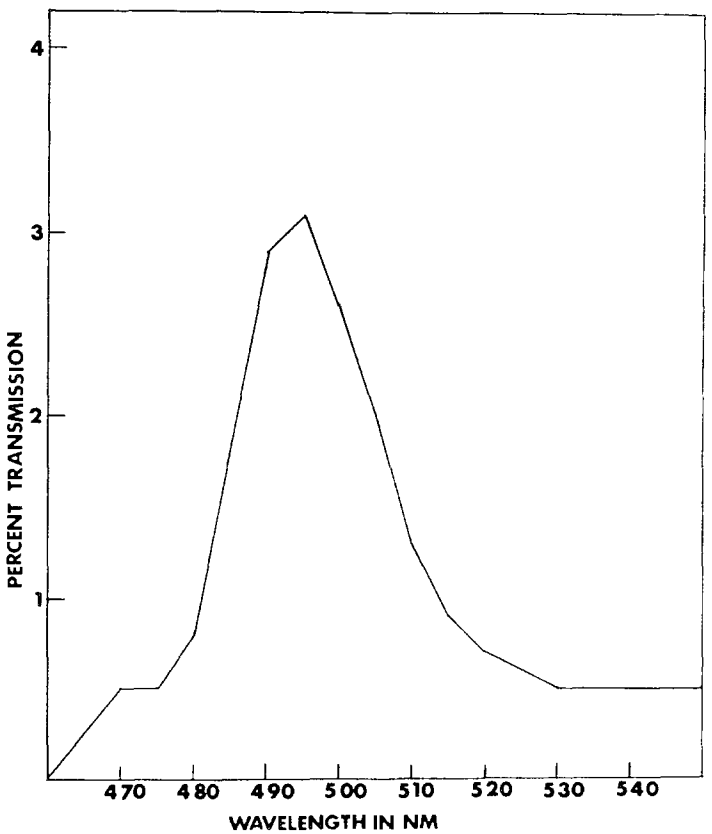

Fig. 1. Transmission curve of the GG 495 and BG 25 filters used with the white light camera at the Vacuum Tower Telescope.

'time available' basis. Because of poor seeing on August 7, other observations were suspended and the routine sunspot photographs were started at about 1520 UT with the shutter triggered manually in moments of better-than-average seeing. Manual observations stopped sometime before 1523 and automatic exposures started at 1524:00 UT. Fortunately, the shutter mechanism malfunctioned; we obtained photographs at approximately a 10 s rate instead of the planned 20 s rate. Observations continued until 1945 UT.

2. Observations

The first 10 min of the flare are poorly recorded. Examination of the Hilltop patrol frames at 1500, 1510 and 1520 UT shows no emission at 1500, possibly a small patch of emission at 1510 and several definite patches at 1520 UT. Detailed analysis of the films began with the pictures at 1520 UT.

2.1. Light curves and a timing problem

The first 26 frames of the Tower Telescope film were triggered at moments of good seeing after 1520 UT and no record was made of the precise time of the first exposure or of the interval between subsequent exposures. After the observations, we reinacted the observing sequence and concluded that the first frame was taken within 1 min after the nominal start time of 1520 UT and that the 26th exposure must have been completed before 1523 UT. Figure 2 shows the 26th exposure, the best of the series. The resolution is 1–2″.

Using a high-resolution microphotometer, we digitized the brightness within a 32″ × × 46″ area on all frames showing flare emission. The size of the microphotometer slit and of the steps between measurements in each direction was 0.5″. Figure 2 shows the area scanned. Brightness in the flare knots was calibrated in terms of the intensity of the photosphere near the center of the scanned area. Figure 3 shows a plot of the brightness of the largest knot vs time on the assumption that the 26 exposures were made at a constant 7 s rate between 1520 and 1523 UT. In addition to the brightness of the knot at 4950 Å, the figure also shows brightness at 5900 Å (from the Hilltop films) and the 60–100 keV X-ray signal recorded on the Intercosmos 7 satellite as well as the microwave emission recorded at Sagamore Hill.

Since manual exposures are generally separated by at least 2 s, and since we know that the 26 exposures were taken between 1520 and 1523, we can establish that the white light maximum occurred at 1522:30 ± 1:00. This time is in close agreement with the microwave and hard X-ray maxima, and it is about 7 min before Hα maximum. This result is in agreement with previous white light flare observations (McIntosh and Donnelly, 1972).

Having established the correspondence between the peak in the 60–100 keV X-ray emission and the white light emission, we used the ESRO TD-1A satellite observations of the 60–87 keV X-rays (van Beek *et al.*, 1973) to examine the possibility that the white light and the X-ray emissions could be very closely correlated as one might expect if both emissions are associated with sub-relativistic electrons impacting on

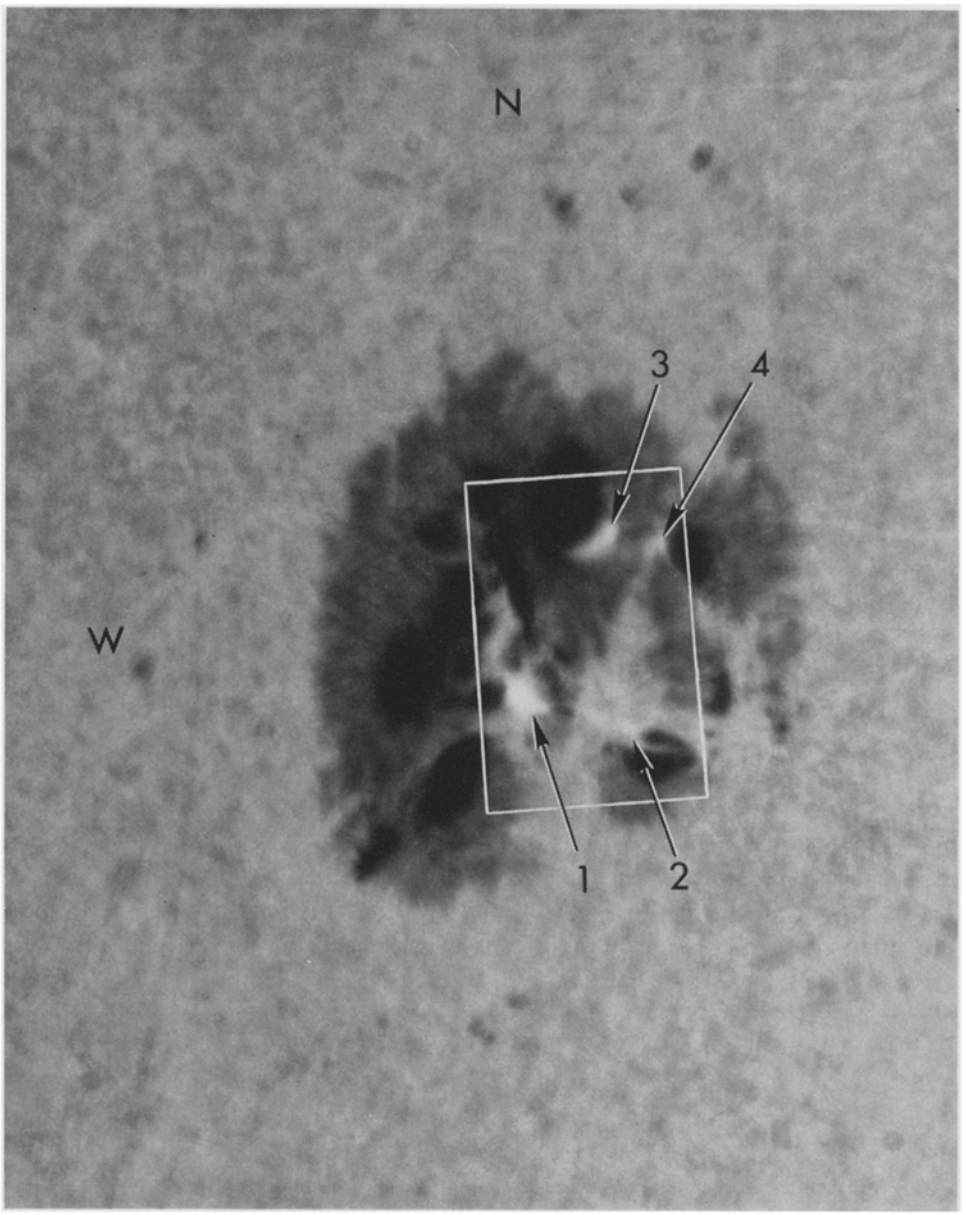

Fig. 2. The white light flare at maximum brightness. Resolution is 1″–2″. The numbered arrows point to the brightest knots. Knot 1 was 50% brighter than the photosphere nearby. The white rectangle outlines the area that was microphotometered for detailed analysis.

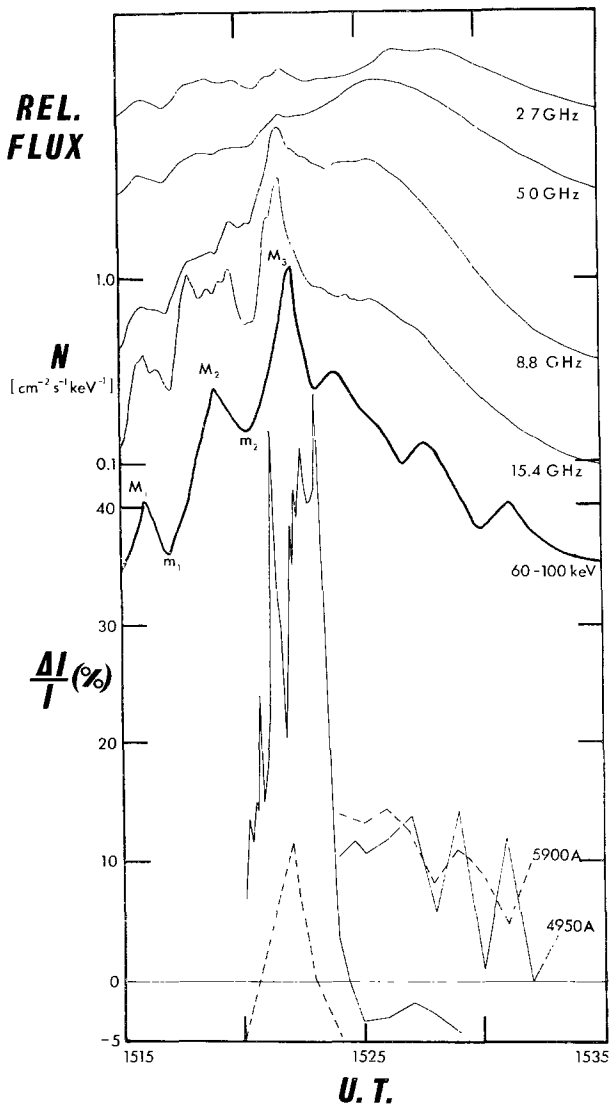

Fig. 3. White light emission curves at 4950 and 5900 Å (bottom) compared with X-ray (middle) and microwave (top curves) emissions. Up to 1524 UT the curves show the temporal behavior of the emissions from the 4 knots shown in Figure 2. After that, the curves refer to the emission associated with the white light wave.

the chromosphere. Since the time base for our observations was uncertain, we allowed the interval between observations to vary under the combined constraints that the 26 observations took place between 1520 and 1523 and that at least 2 s were required to take each exposure. We computed cross-correlations between the X-ray count rate (time resolution smoothed to 2 s) and the 4950 Å intensity in the large knot. The other three knots were not considered separately because their brightness varied with time

in the same way as the brightness of the largest knot. The morphology of the flare will be described in more detail in Section 2.2.

Under the timing constraints mentioned above, the minimum cross-correlation between the visible and X-ray emissions was 0.55. The maximum correlation was obtained when we took into account the fact that there must have been several seconds lost after the 5th, 10th, and 15th exposures as the exposure setting was changed. Assuming an otherwise uniform exposure rate of 2 s from 1520:40 to 1521:42, we find a correlation of 0.91 with 95% confidence limits at correlations of 0.96 and 0.81. This close similarity between the visible and X-ray emission curves is shown graphically in Figure 4. Of course, uncertainty in timing clouds the precision of this result. How-

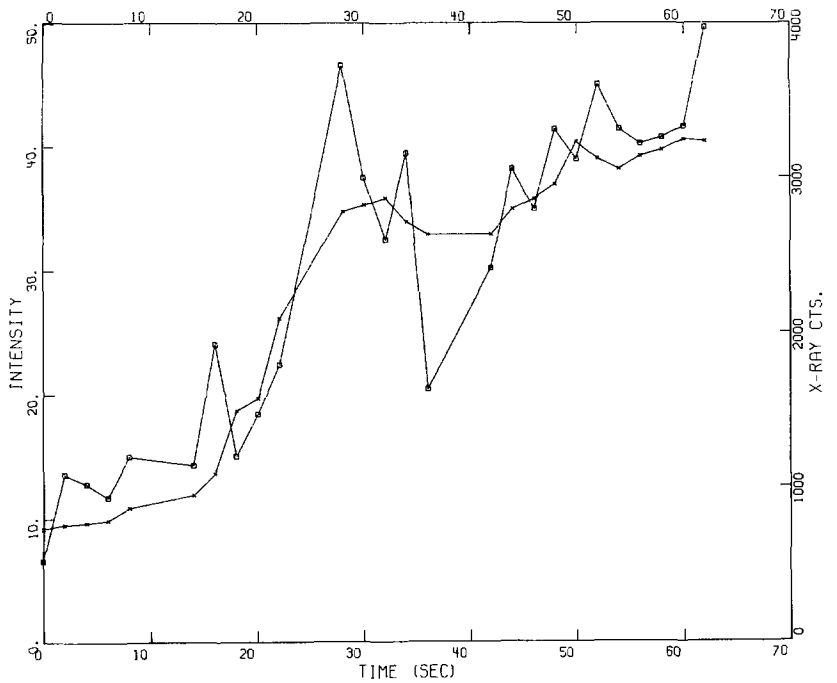

Fig. 4. White light (–□–□–□–) and X-ray (–×–×–×–) emission curves vs time. T_0 is 1520:40 UT.

ever, the correlation remains above 0.70 in the region of most plausible timing for the 26 exposures, and even if a least squares straight line is removed from each curve, the data still indicate a high (0.54) correlation between the X-ray and white light fluctuations. This result is in agreement with those of Zirin and Tanaka (1973) and of Vorpahl (1972) who found a close correspondence between hard X-rays and the hydrogen line emission in flare knots.

A linear least squares fit of the X-ray count rate to the 4950 Å light curve yields the following relation:

$$I(4950) = 2.42 + 0.012\, I(60\text{–}100 \text{ keV}),$$

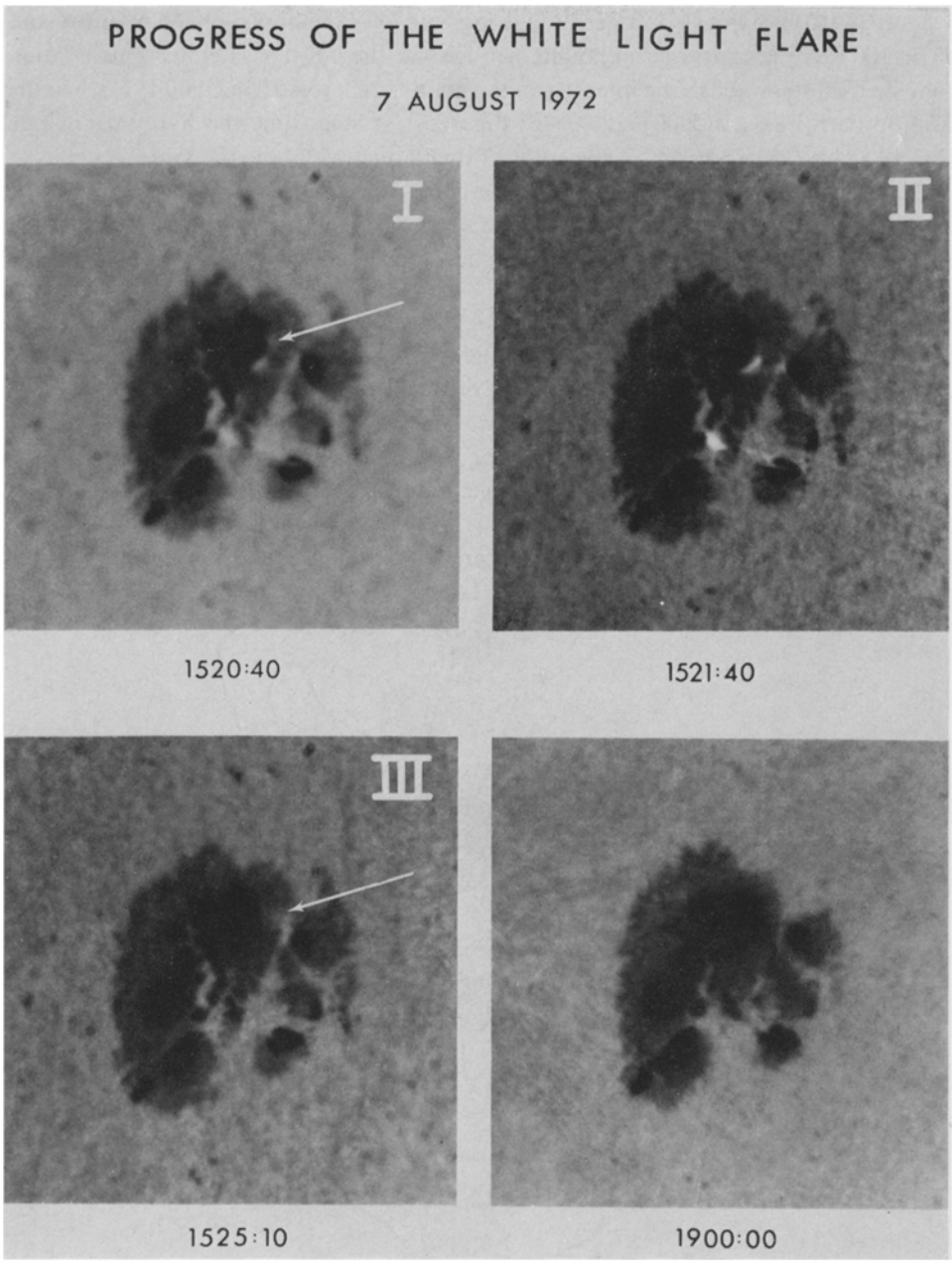

Fig. 5. Progress of the white light flare through three phases. The white arrows point to the knot that was fading at 1520:40 and to the faint wave at 1525:10.

where $I(4950)$ is expressed in percentage increase over the photospheric intensity and $I(60\text{–}100$ keV) is expressed in counts per 1.2 s at the TD-1A satellite. This relation may be used to establish the intensity in the main flare knots at 1522:00 UT, when the Hilltop patrol gave $I(5900)=11\%$ (see Figure 3). At that time the X-ray count rate was 1900, so $I(4950)\cong 25\%$, if the color of the flare at 1522 was the same as it was at 1521:42 when the last of the Tower Telescope exposures was made and when the knots were near peak brightness. *This means that the knots had a very bluish spectrum*, much more so than the spectrum of the phase that immediately followed.

2.2. Bright knots and a white light wave

Since the August 7 observations are unique in their spatial and temporal resolution, a detailed description of the development of the optical emissions is in order.

As shown in Figure 5, the first clear view of the white light emission (at 1520:40 UT) revealed at least 5 faint patches, including one (marked with a white arrow in the upper left panel) that had faded by flare maximum (1521:40 in the continuum and in X-rays). On the Hilltop patrol films, there is a suggestion of this patch at 1510. As the emission increased, the other 4 centers of emission retained their outlines: two knots

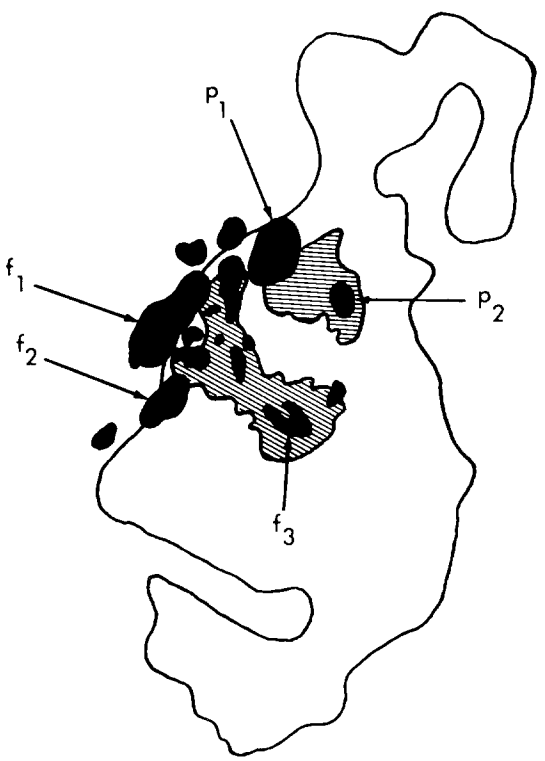

Fig. 6. Comparison of sunspot locations, Hα and D_3 emissions. The black line shows the extent of the Hα emission at flare maximum (1529 UT). The shaded area indicates where the brightest helium D_3 emission occurred. Black patches (marked p_1, f_1, etc.) are sunspots. Notice that the helium emission was confined to a much smaller area than the Hα emission, but that it covered a larger area than the continuum emission (compare with Figure 5).

at the inner boundaries of the penumbrae of spots p_1 and p_2 (see Figure 6 for spot designations) connected by a faint bridge, and in the south, two knots similarly connected by a faint emission bridge between spots f_3 and the southeastern edge of spot f_1. The bright knots all lay within a few arc sec of umbrae. Notice that the emission extended into the umbra of spot f_3 along a light bridge that seems otherwise to have been unaffected by the flare. The brightest knot is marked '1' in Figure 2, and it lay over an area that was about 5% darker than the surrounding photosphere before and after the flare. The knots between p_1 and p_2 lay over penumbrae. The emissions in the p area and in the f area were equidistant from the neutral line of the longitudinal magnetic field, which was mapped at 1632 UT (Rust and Bar, 1973). The distance from the $B_{\parallel}=0$ line to a line joining the two knots in the p area, for instance, was about 10000 km and it remained unchanged during that phase of the flare. The white light patches were not intersected by the neutral line.

The knots seen in the first 26 frames have typical dimensions of $3'' \times 5''$ (see Table I). Seeing does not affect this measurement on the best frames. There is no evidence for motion or change in size of the knots before the gap in observations between 1523 and 1524 UT. The pictures starting at 1524:00, however, show that all the knots had faded to near invisibility while the bridge connecting spots p_1 and p_2 had moved $5''$ (3600 km) northward. This was the beginning of a *white light wave* that moved outward, roughly perpendicular to the neutral line. The wave is faintly visible in the 1525:10 photo of Figure 5. It moved northward across the penumbrae of spots p_1 and p_2 and into the photosphere at a velocity of 30–40 km s^{-1} until 1529, when it slowed to a few km s^{-1}. Comparison with the Hα developments shown in the Big Bear Solar Observatory photograph (Figure 7) reveals that the white light wave front coincided with one part of the leading edge of the Hα ribbon as it grew during the flash phase. Křivský *et al.* (1973) studied the development of this flare in detail, and their result for the Hα ribbon velocity (50 km s^{-1}) agrees well with ours, considering that they probably chose a different (unspecified) part of the expanding ribbon to measure. The wave was seen very clearly in the northernmost ribbon, and when the film is projected at 24 frames s^{-1}, the eye can detect a faint wave moving southward from the bright knot '1' near spot f_1. The velocity is $\sim$40 km s^{-1} although this wave is too faint to be discerned on individual frames and precisely measured.

Until about 1537 UT, the northern part of the wave is clearly visible as a $3''$ wide dark smudge on the Tower Telescope negatives. Maximum visibility is between 1530 and 1531 UT. As shown in Figure 3, the brightness of the wave (11% brighter than the photosphere) is about the same on the Hilltop patrol film at 5900 Å as on the Tower films at 4950 Å. *The flat spectrum and the motion of the wave clearly distinguish it from the stationary, bluish knots that appeared earlier in the flare.*

2.3. Three phases in the emission curves

Figures 3 and 4 show how closely the chronologies of the white light knots and of the wave resemble those of the hard X-ray and microwave bursts. Křivský *et al.* (1973) discussed the August 7 flare in terms of a gradual onset (before 1508 UT), an im-

Fig. 7. Progress of the white light wave over the Hα flare region. Successive positions of the wave front between 1525 and 1532 are marked. The Hα picture shows the flare at 1533 UT (BBSO photograph).

pulsive phase (1508–1516 UT), and an explosive phase (1516–1527 UT). However they were unable to detect any unique relations between X-ray or radio flux maxima and the optical events. The present data make it possible to pinpoint at least three developments during the explosive (or flash) phase that help to outline the course of particle acceleration in the flare. We label the phases I–III.

At 1520 UT the hard X-ray detectors showed emission decreasing from a peak (M_2 in Figure 3) at 1518:45 (Phase I). Similarly, in white light at 1520:40, one knot was decaying (see Figure 5). Meanwhile, the emission knots 1–4 were brightening (Phase II), and the peak brightness was simultaneous (ref. Section 2.2) with the hard

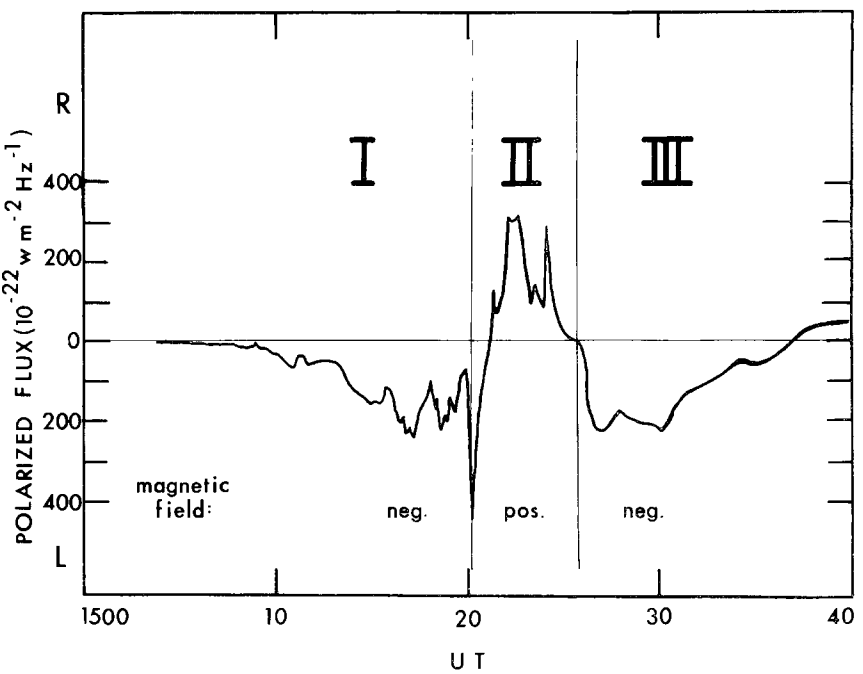

Fig. 8. Polarized radio flux vs time. The thin vertical lines show where the flare may be divided into Phases I–III on the basis of the polarity of the magnetic field from which the brightest emissions arose.

X-ray peak M_3 at 1521:40. Both white light emission and hard X-ray emission fell sharply in the next two minutes. The next X-ray maximum (beginning of Phase III) was at 1524, near the time when the white light wave must have started. The wave seemed to brighten at 1530–1531: this is reflected in the peak in X-ray flux at 1531. We conclude that despite the uncertainties in our measurements, the results shown in Figures 3 and 4 imply that there was a near 1:1 correspondence in time between white light and hard X-ray emissions and that *separate peaks in the X-ray flux curve may be related to separate patches that brighten sequentially in the course of the flare.*

This identification of particular flare patches with peaks in the X-ray flux curve is supported by analysis of 9.4 GHz radio emission polarization measurements from

Huancayo. Figure 8 shows how the sense of circular polarization reversed from R to L between 1520 and 1521 UT, i.e., at the beginning of Phase II. The sense of polarization reversed again between 1524 and 1525, when the wave of Phase III started. Comparison with the sequence of events pictured in Figure 5 will show that the period when the microwave emission was right-circularly polarized coincided with the phase of visible emission from near spots p_1 and p_2. The field in these spots is downward directed (negative), and we expect that magnetobremsstrahlung at 9.4 GHz in a negative field will be right-circularly polarized. At 1520:40, the emission from the negative spots was waning and the large knot in the midst of the (positive) *f* spots was brightening. This is Phase II and we may anticipate the change in polarity from R to L in the microwaves. Then, the wave of Phase III passed over penumbrae of (negative) *p* polarity. The return to R polarization at 9.4 GHz coincided with the dominance of the wave from 1524 to 1537 UT. These results agree with those obtained by Nefed'ev (1973) and by Énomé and Tanaka (1973), who used much lower resolution observations to infer that the sense of polarization in complex microwave bursts varies with time because the brightest portion of the burst moves across regions of differing magnetic polarity.

To further establish the correspondence between the region of microwave emission and the optical flare sites, we computed the cross correlation between the amount of polarization and the intensity at 4950 Å during Phase II. The cross correlation is 0.73.

The white light wave (Phase III) appears to have an analog in the microwave burst intensity profiles (see Figure 3). At 1526 UT a secondary peak appeared at the highest frequencies and it shifted to lower frequencies during the next 4 min. Hagen and Barney (1968) suggested that such a drift in the microwave burst may be interpreted as an effect of an outwardly expanding plasma cloud. Using their method of analysis, we find an average outward velocity of the same order of magnitude as the white light wave velocity.

Finally, we studied the structure of the flare in Hα and in the D_3 line (5876 Å) of helium (Figure 6). The bright kernels of hydrogen emission discussed by Zirin and Tanaka (1973) coincided with two of the knots that appeared during Phase II. Hydrogen alpha emission did not appear at the kernels until about 1520 UT, i.e., when the sense of polarization at 9.4 GHz shifted from L to R. Just prior to 1520, the Hα flare was brightest in the area between spots p_1 and p_2, i.e., where we photographed the fading white light emission at 1520:40 UT. Later expansion of the Hα ribbons in this area coincided with the path of the white light wave.

A helium D_3 spectroheliogram made at 1524 confirms the fact that the hottest part of the chromospheric flare coincided with the white light emission.

2.4. Source of the emission

Machado and Rust (1974) studied the spectrum of the flare wave and they gave a temperature estimate of 8500 ± 500 K. This is an extraordinary temperature in comparison with the few hundred degree temperature excess that has been predicted by Švestka (1970) and by Najita and Orrall (1970). The predictions were based on the

assumption that the white light flare takes place in the photosphere near $\tau = 1$. Machado and Rust concluded that the emission in the wave came instead from an optically thin cloud between $\tau = 0.1$ and $\tau = 0.01$, and they used intensity measurements from the filtergrams to conclude that the bright knots of Phase II might represent a superposition of emissions from hot layers near $\tau = 0.1$ and from a slightly overheated photosphere at $\tau = 1$. However, any such conclusion may be incorrect if the emission shown in the filtergrams is contaminated by line emission.

The only strong line within the passbands of the filters is the Hβ line at 4861 Å. Fortunately, spectra are available to estimate the possible effect of this line on the observations. In the area of the white light wave, spectra from BBSO and from SPO show that Hβ and Hα are only 1–2 Å wide. They are not important contributors in filtergrams with 175–250 Å passbands. The situation in the bright knots is different, however. Zirin and Tanaka's (1973) spectra show that at 1520 UT Hα had an equivalent width of 10 Å in the brightest knot. No spectra of the knots in Hβ are available; however, Hβ usually has an equivalent width comparable to that of Hα (Smith and Smith, 1963). If one assumes that Hβ had an equivalent width of 20 Å at white light maximum, then one may readily use the filter transmission curve (Figure 1) to compute a maximum Hβ contribution of 5% over the apparent photospheric brightness. The maximum measured increase over the photosphere was 50%, so we conclude that Hβ is not an important contributor to the observed emission. It is of the order of our estimated errors in photographic photometry.

2.5. Error estimates

It is difficult to estimate the errors in photometering the knots since the seeing was varying rapidly between 1″ and 5″ from one frame to the next. Also, the exposure times at the Tower Telescope varied due to a defective shutter mechanism. Further, if we accept the high correlation between the 4950 Å emission and the hard X-ray intensity, the error estimates are further complicated by the presence of real brightness variations within seconds.

An empirical estimate of the errors may be obtained by supposing that the brightness of the Phase III wave varied slowly compared to the exposure interval of 10 s. Then, a glance at the right hand side of Figure 3 will show that the errors in measuring the peak intensity of 3″ features on the Tower Telescope film must have been on the order of $\pm 5\%$ of the photospheric brightness. The errors at 5900 Å are estimated to be $\pm 2\%$, because the seeing and the exposure time at the Hilltop Telescope were more stable than at the Tower.

3. Energy Estimates

From intensity and area measurements for Phases II (knots) and III (wave), we may estimate the energy of the visible continuum. Table I shows the area of each of the 4 knots and of the wave and the peak intensity of each feature relative to the surrounding photosphere. The table also gives the emission rates at 4950 Å and at 5900 Å at

TABLE I

Continuum emission rates

Phase II (~1522 UT)	Knot	Near spot	Area (10^{17} cm^2)	$I_{flare}/I_{photosphere}$		Emissivity (erg cm^{-2} s^{-1} Å^{-1})	
				4950	5900	4950	5900
	1	f_1	1.36	0.50	0.11	6.8×10^6	1.4×10^6
	2	f_3	1.04	0.26	0.06	3.5×10^6	0.8×10^6
	3	p_1	1.04	0.48	0.11	6.5×10^6	1.4×10^6
	4	p_2	0.38	0.21	0.08	2.9×10^6	1.0×10^6
	3–4	p_1–p_2	2.08	0.19	0.11	2.6×10^6	1.4×10^6
Phase III (1527:00 UT)	Wave						
	3–4	p_1–p_2	2.08	0.11	0.11	1.5×10^6	1.4×10^6

the peak brightnesses. Limb darkening and foreshortening have been taken into account in the figures. Extrapolating the spectral curves of the knots and of the wave over the visible range (3900–6900 Å), we arrive at the following estimates for the emission rates:

knots 1 and 3

14.6×10^9 erg cm^{-2} s^{-1} × area = 35×10^{26} erg s^{-1}

knots 2 and 4

7.9×10^9 × area = 11×10^{26}

wave

4.4×10^9 × area = 9×10^{26}.

We have treated knots 1 and 3 separately from knots 2 and 4, since the results shown in Table I indicate that the first two knots had about equal emission rates, as did the last two knots. This result, which is not evident from examination of Figure 2, tends to support the view expressed by Rust and Bar (1973) that emission knots that lie equidistant from the line of zero longitudinal magnetic field represent conjugate points on magnetic field loops overlying the flaring region. Knots 1 and 3 were opposite each other in the western portion of the white light flare, and knots 2 and 4 were similarly equidistant in the eastern part of the flare. It should be mentioned that, in computing the brightness of the flare knots, we have assumed that the flare emission was optically thin so that the brightness of the underlying photosphere must be subtracted from the measured flare brightness. The ratios of flare brightness to photospheric brightness were found according to the following formula:

$$\frac{I_{\text{flare}}}{I_{\text{photosphere}}} = \frac{I_{\text{measured}} - I_{\text{penumbra}}}{I_{\text{photosphere}}},$$

where I_{penumbra} refers to the intensity of whatever was beneath the flare knot under study. In particular, knots 3 and 4 covered penumbrae, knot 1 covered an area that was 5% darker than the nearby photosphere, and knot 2 lay over the photosphere and along a light bridge of photospheric brightness.

A comparison of the above emission rates with the Hα emission rate computed by Zirin and Tanaka (1973) shows that the visible continuum and the Hα emission rates were comparable, but that, because of the much larger area and lifetime of the Hα emission, the total energy radiated in the line was somewhat more than the energy from the visible continuum. In particular, if we take the half-life of the knots to be 90 s, they account for 5.8×10^{29} erg. The emission from the wave, at a half life of 450 s, amounted to 4.0×10^{29} erg. The total energy emitted in the visible continuum (9.8×10^{29} erg) was about one-third the energy that Zirin and Tanaka estimated was lost by Hα radiation.

4. Conclusions

We have found a close correlation between the visible continuum, which is due to thermal emission in the upper photosphere – lower chromosphere region, and hard X-ray and microwave bursts, which are due to non-thermal emission processes. August 7, 1972 was the first time that white light flare observations with good time resolution became available and the analysis described in Section 2.1 showed that fluctuations in the X-ray intensity, even on a time scale of a few seconds, were statistically correlated with the intensity of the white light emission. According to Machado and Rust (1974) the white light emission of what we have herein called Phase III of the flare came from low in the atmosphere, near $\tau = 0.1$, which is about 400 km above the top of the photosphere. The ambient electron density at that level was about $3 \times \times 10^{13}$ cm^{-3}. According to van Beek *et al.* (1973) the hard X-rays originated in a plasma layer with an ambient density higher than 2×10^{10} cm^{-3}. In the normal solar atmosphere, these levels are separated by less than 2000 km, so we conclude that the *white light and hard X-ray emission patches must have been nearly cospatial.* The close temporal correspondence between fluctuations in the two forms of emission supports this result. Thus, we may conclude that the hard X-ray emission patches were only 3″–5″ across. This result confirms balloon observations of a large flare in which Takakura *et al.* (1971) were able to place an upper limit of 1′ on the hard X-ray source size.

In many ways the observations of this flare confirm earlier work on white light flares (Stover and DeMastus, 1967; McIntosh and Donnelly, 1972; Michard, 1959). White light maximum occurred 7 min before Hα maximum, and the 4 knots seen then were bluish, stationary and on the edges of sunspot umbrae. However, the present observations show that the white light event was quite complicated, and we have found it convenient to divide it into three phases. During the first phase we have inferred that a patch of emission occurred over the penumbra of a negative sunspot while the hard X-rays and microwaves reached a peak at about 1518 UT. The microwave emission at the time was left-circularly polarized, indicating magnetobremsstrahlung emission from relativistic electrons in a negative magnetic field. The maximum in these Phase I emissions was accompanied by a Type II metric burst (Dodge, 1973).

Two interesting features emerge from study of the emissivities of the 4 knots of Phase II. The emission rates in individual pairs of knots on opposite sides and equidistant from the boundary between positive and negative magnetic fields were equal.

We infer that particles were being accelerated in roughly equal numbers down both legs of a tubular magnetic loop with a 2500 km cross section and a 10000 km radius of curvature. This conclusion applies to the central parts of the 4 knots only, since, when the total area of the patches on each side of the magnetic border is taken into account, there is more emission from the positive field side than from the other side. This excess of emission from the positive side corresponds to an excess of right-circularly polarized 9.4 GHz emission during this phase of the flare. It is interesting to speculate that the magnetic field changes discussed by Rust (1973) may have caused changes in the heights of the mirror points for some of the particles in the magnetic loops connecting the positive and negative spots.

By our discussions in previous sections we have implied that the same non-thermal electrons that were responsible for the X-rays and 9.4 GHz magnetobremsstrahlung were also responsible for heating the white light emission region. Indeed, we find in our observations considerable evidence for Brown's (1973a, b) electron heating models. Although Machado and Rust (1974) were unable to deduce the vertical structure of the bright knots of Phase II, they concluded that the Phase III emission came from a thin layer with $n_e = 3 \times 10^{13}$ cm^{-3} and $T = 8500$ K. In Brown's models, such an emitting layer would be produced by a beam of electrons with energies between 20 and 100 keV. The intensity of the beam would be 10^{11} erg cm^{-2} s^{-1} and the spectral index $\delta = 5$. Presumably the more intense emission from the Phase II knots was caused by an electron beam of even higher energy density and lower spectral index. In fact, the data of van Beek *et al.* (1973) show that the spectral index of the electron beam responsible for the hard X-rays was 4.5 during Phase II and 5.2 during Phase III (thick target model assumed; see Brown (1973b)).

We do not need to consider heating of the flaring layers by protons because energy in the electron beams inferred above is already an order of magnitude more than adequate and because Hudson (1973) has shown that heating due to protons will be very much diluted relative to that due to the electrons. The proton range of energy deposition greatly exceeds that of the electrons. Brown's models may have to be modified somewhat to account for the apparent low emissivity in the visible continuum. Perhaps most of the energy in the impacting electron beam is emitted in the EUV flash (Donnelly, 1971) from regions where $n_e \approx 10^{12}$ cm^{-3}.

Phase II ended with the abrupt fading of the 4 stationary knots. The next phase was characterised by a softer X-ray spectrum, another type II radio burst, and a return of the white light emission to negative fields (the microwave polarization reversed, too). The white light emission took the form of an outward moving wave. We conclude that the acceleration region was a cylindrical section expanding at about 40 km s^{-1}. The white light wave appears to have been the locus of points where the expanding acceleration zone intersected the chromosphere. Our comparison of the wave trajectory with the Hα flare showed that the wave coincided with the leading edge of the flare ribbon, and we emphasize that the white light wave bore no similarity to a Moreton (1961) wave, which is usually interpreted as a shock wave and which moves outward at 1000 km s^{-1}. No Moreton wave was detected in association with the August 7 flare.

Because the X-ray spectrum softened and the emissivity in the visible continuum decreased to only 4.4×10^9 erg cm^{-2} s^{-1}, we conclude that the particles accelerated in Phase III were not so energetic as those of Phase II. However, it is important to note that the white light emission continued until about 1540 UT – long after Hα maximum. This is consistent with the persistence of hard X-ray and non-thermal microwave emission until then, and it shows that particle acceleration did not stop at flare maximum. The slow fading of the wave and the slow disappearance of the non-thermal emissions imply that the acceleration mechanism did not shut off abruptly in Phase III, but rather that it slowly weakened to below the point of perceptability.

Acknowledgements

We are grateful to Horst Mauter, J. E. Coleman and Lou Gilliam of the Sacramento Peak Observing Staff for their help in obtaining the observations. We also thank Dr Harold Zirin for permitting us to examine the Big Bear Solar Observatory films. Dr Joan Vorpahl and Dr Zdeněk Švestka read an early version of the manuscript and made valuable suggestions for improvements, and we have benefitted from discussions with Dr Ron Straka and Dr Donald Guidice of the AFCRL Radio Physics laboratory.

References

Brown, J. C.: 1973a, *Solar Phys.* **31**, 143.
Brown, J. C.: 1973b, *Solar Phys.* **28**, 151.
Coffey, H. E. (ed.): 1973, 'Report UAG-28', WDC-A for Solar-Terr. Physics, NOAA, Boulder, Colo.
Demastus, H. L. and Stover, R. R.: 1967, *Publ. Astron. Soc. Pacific* **79**, 615.
Dodge, J. C.: 1973, in H. Coffey (ed.), 'Report UAG-28', WDC-A for Solar-Terr. Physics, NOAA, Boulder, Colo. p. 242.
Donnelly, R. F.: 1971, *Solar Phys.* **20**, 188.
Énomé, S. and Tanaka, H.: 1973, in R. Ramaty and R. Stone (eds.), *High Energy Phenomena on the Sun*, NASA SP-342, p. 87.
Hagan, J. P. and Barney, W. M.: 1968, *Astrophys. J.* **153**, 275.
Hudson, H. S.: 1973, in R. Ramaty and R. G. Stone (eds.), *High Energy Phenomena on the Sun*, NASA SP-342, p. 207.
Křivský, L., Valníček, B., Böhme, A., Fürstenburg, F., and Krüger, A.: 1973, preprint from the *7th Regional Consultation on Solar Physics*, Starý Smokovec, Czechoslovakia.
Machado, M. E. and Rust, D. M.: 1974, *Solar Phys.* **38**, 499.
Mathews, T. and Lanzerotti, L. J.: 1973, *Nature* **241**, 335.
McIntosh, P. S. and Donnelly, R. F.: 1972, *Solar Phys.* **23**, 444.
Michard, R: 1959, *Ann. Astrophys.* **22**, 887.
Moreton, G.: 1961, *Sky Telesc.* **21**, 145.
Najita, K. and Orrall, F. Q.: 1970, *Solar Phys.* **15**, 176.
Nefed'ev, V. N.: 1973, *Issledovaniya Geomag., Aeron., Fiziki Solntsa* (SibIZMIR), **26**, 143.
Rust, D. M.: 1973, *Solar Phys.* **33**, 205.
Rust, D. M. and Bar, V.: 1973, *Solar Phys.* **33**, 445.
Smith, H. J. and Smith, E. v. P.: 1963, *Solar Flares*, Macmillan, New York.
Švestka, Z.: 1970, *Solar Phys.* **13**, 471.
Takakura, T., Ohki, K., Shibnya, N., Fuji, M., Matsuoka, M., Miyamato, S., Nishimura, J., Oda, M., Ogawara, Y., and Ota, S.: 1971, *Solar Phys.* **16**, 454.
van Beek, H. F., Hoyng, P., and Stevens, G. A.: 1973, in H. Coffey (ed.), 'Report UAG-28', WDC-A for Solar-Terr. Physics, NOAA, Boulder, Colo. p. 319.
Vorpahl, J.: 1972, *Solar Phys.* **26**, 397.
Zirin, H. and Tanaka, K.: 1973, *Solar Phys.* **32**, 173.